Materials Letters 65 (2011) 3336–3339

Contents lists available at ScienceDirect

Materials Letters

journal homepage: www.elsevier.com/locate/matlet

Optical and electrical properties of ink-jet printed indium–tin-oxide nanoparticle films

Hsiang-Yu Lai, Tsung-Han Chen, Chun-Hua Chen *

Department of Materials Science and Engineering, National Chiao Tung University 1001 Ta-Hsueh Road, Hsin-Chu 30010, Taiwan, ROC

ARTICLE INFO

Article history:
Received 1 May 2011
Accepted 18 July 2011
Available online 22 July 2011

Keywords:
ITO
Nanoparticle
Ink-jet printing

ABSTRACT

In this work, spherical indium tin oxide (ITO) nanoparticles (~15 nm) synthesized by co-precipitation method were successfully applied for direct ink-jet printing of transparent conducting patterns on polyethylene terephthalate substrates. The printed ITO nanoparticle patterns with various thicknesses were investigated for understanding fundamental properties and potentials for soft electronics. It has been found that the optical transmittance in the visible region as well as the band-gap absorption edge of the printed ITO films significantly varies with thickness, which is related to the huge nanoparticle scattering effect as evidenced. The electrical resistivity can be effectively improved by increasing the pattern thickness, indicating that the present printed ITO films are of great potential for optoelectronic applications.

1. Introduction

In_2O_3:Sn (indium tin oxide, ITO), an important transparent conducting oxide, has been widely studied and applied as transparent electrodes for many optoelectronic devices [1–3]. For most applications, ITO films are deposited on rigid substrates by gas-phase deposition, such as magnetron sputtering, chemical vapor deposition, and spray pyrolysis [4–6]. The deposited high-quality ITO films generally have a low electrical resistivity of ~10^{-4} Ω-cm and at least 85% transmittance in visible region [7]. However, the requirements of the high-cost equipment and complicated patterning processes are the major demerits for these deposition techniques. Developing potential alternative technologies with low costs and simple processes are thus considered an important research topic not only for replacing the conventional ITO procedures but also for providing further possibilities in nanotechnology-related applications.

The ink-jet printing method is one of the most potential techniques for manufacturing electrodes by direct printing transparent conducting materials onto substrates without any patterning and etching processes. Although ink-jet printing of the conducting polymer ink or special composite ink consisting of metallic particles and organic solvents has been well demonstrated [8,9], studies on the ink-jet printing of ITO nanoparticles are extremely lacking [10,11].

In this letter, we report the successful ink-jet patterning of ITO nanoparticles on flexible substrates and the significant thickness dependences of the optical and electrical properties. For this purpose, we synthesized ITO nanoparticles with a spherical shape and designed chemical composition by a relatively common, rapid, low-cost, and reliable technique, i.e. the co-precipitation method, which allows for the easy tuning of the nanoparticle size, composition and especially the yield. To our knowledge, the method is the first time to be introduced for the preparation of the ITO nanoparticle ink. The designed patterns were then fabricated by direct printing of the prepared ITO nanoparticle ink on flexible substrates and the pattern thickness was well controlled with printing cycles. The relation between the agglomerate ITO nanoparticles and the thickness dependences of the optical and electrical properties was also addressed.

The present letter incorporates several new points including the synthesis of high-yield and uniform ITO nanoparticles, policy for the low nanoparticle concentration and repeated printing for obtaining designed thickness (instead of the concentration controlled thickness), and most importantly provides distinct nanoparticle dependent results for understanding of fundamentals and potentials for optical and electronic applications.

2. Experimental procedures

Indium chloride ($InCl_3 \cdot 4H_2O$, 1.00 g) and tin chloride ($SnCl_4 \cdot 5H_2O$, 0.13 g) were dissolved to 50 ml of distilled water as the starting solution. The ammonia solution (NH_4OH) was then dropped into the starting solution under stirring to keep a constant pH value of 10. After aging for 3 h, the white precipitation was collected and dried. The dried precipitation was heated to 700 °C for 3 h to obtain ITO nanoparticles. The ITO ink was synthesized by dispersing the ITO nanoparticles in an ethanol/methanol mixed solution with a solid content of 0.5 wt.%. The printing process was demonstrated on flexible substrates (Polyethylene terephthalate, PET) by a modified ink-jet printer (HP Deskjet 3940). The crystal structures were identified by X-ray diffraction (Bruker, D2

* Corresponding author. Tel.: +886 35 131 287; fax: +886 35 724 727.
E-mail address: ChunHuaChen@mail.nctu.edu.tw (C.-H. Chen).

0167-577X/$ – see front matter © 2011 Elsevier B.V. All rights reserved.
doi:10.1016/j.matlet.2011.07.046

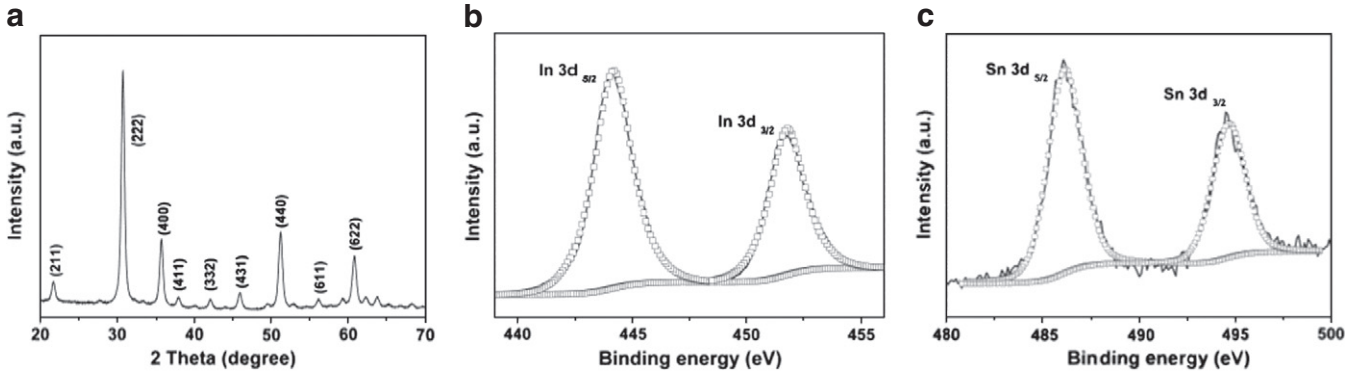

Fig. 1. (a) The XRD pattern and the corresponding XPS spectra of (b) In 3d and (c) Sn 3d band of the as-synthesized ITO nanoparticles by co-precipitation method.

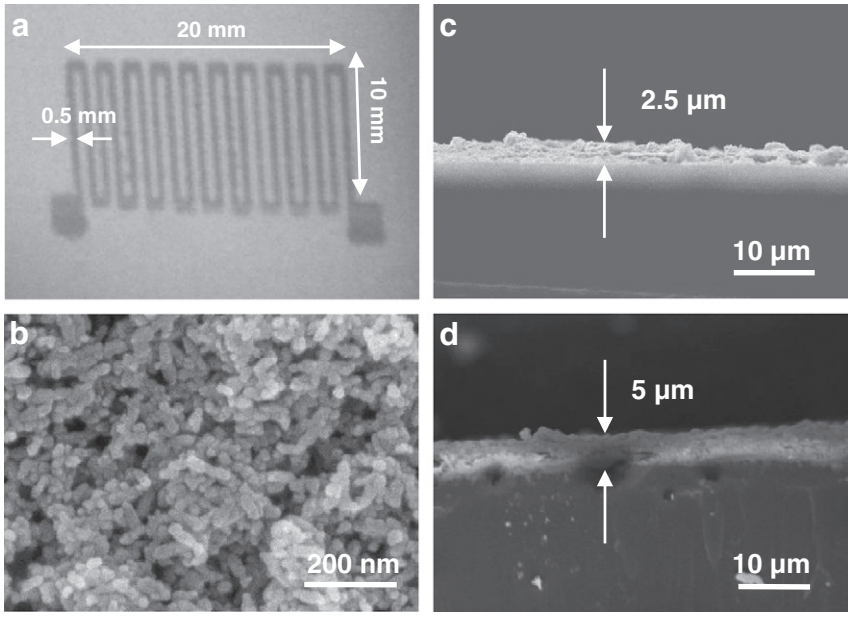

Fig. 2. (a) One printed ITO nanoparticle pattern for 10 printing cycles, (b) the SEM planar view of the printed films, and the SEM cross-section view of the printed films for (c) 5 and (d) 10 printing cycles.

phaser diffractometer). The chemical state and In-to-Sn atomic ratio were determined by an X-ray photoelectron spectrometer (XPS) (Thermo VG Scientific) employing monochromatic AlK_α source (1486.6 eV). The surface morphology and thickness of the printed films were characterized by field emission scanning electron microscopy (SEM) (JSM 6700F). The topography was imaged by atomic force microscopy (AFM) (Veeco Innova SPM) and the root mean square (RMS) roughness was calculated. The optical transmittance of the film was measured by a UV–visible spectrometer (Evolution 300). The electrical resistivity of printed films was measured with a 4-probe method (CMT-SR 2000N).

3. Results and discussion

Fig. 1(a) shows the XRD pattern of the prepared ITO nanoparticles. As can be seen, all the diffracted peaks can be indexed with the cubic bixbyite structure of In_2O_3 (JCPDS 06–0416). The lattice parameter calculated from the XRD patterns was 10.123 Å, which is larger than the JCPDS value of 10.118 Å for the In_2O_3 powder. This increase in lattice constants of the ITO nanoparticle films can be explained by the incorporation of Sn ions into In sites. The crystalline size estimated by Debye–Scherrer equation from a full-width at half-maximum (FWHM) of (222) peak is ~15 nm. Fig. 1(b) and (c) show the XPS spectra of the In 3d and Sn 3d band, respectively. A doublet peak found at 444.2 eV and 451.8 eV is correspondingly attributed to In $3d_{5/2}$ and In $3d_{3/2}$ of In_2O_3. The binding energy of Sn $3d_{5/2}$ and Sn $3d_{3/2}$ located at 486.1 eV and 494.6 eV is corresponded to Sn^{4+} state for SnO_2 doped in ITO and is in

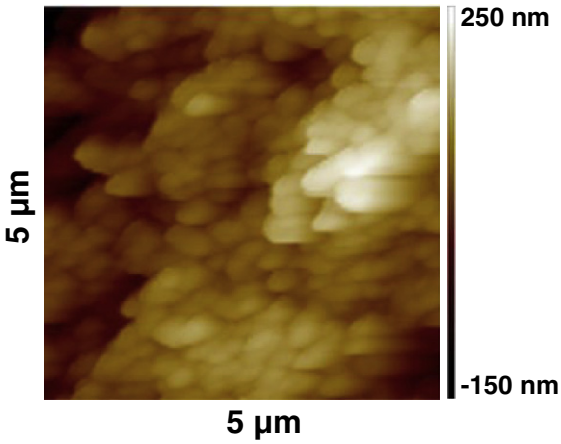

Fig. 3. The AFM height image of the ink-jet printed film (5 printing cycles).

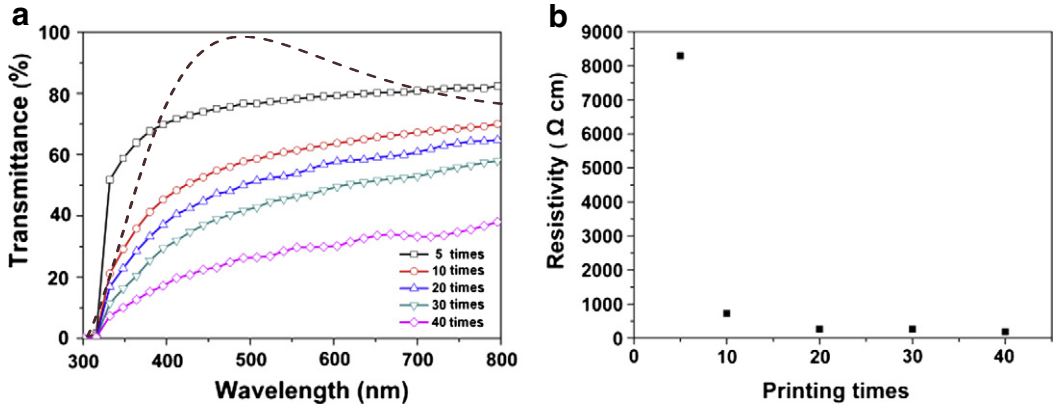

Fig. 4. The printing cycle dependence of (a) the optical transmittance and (b) the electrical resistivity of the ink-jet printed ITO nanoparticle films. The dash line indicates the calculated transmittance of 15 nm ITO nanoparticles.

agreement with the results reported [12]. The In-to-Sn atomic ratio obtained from the measured In $3d_{5/2}$ and Sn $3d_{5/2}$ peaks indicates that the Sn dopants is ~15 at.%, which is consistent with the value analyzed by energy dispersive X-ray Spectroscopy.

Fig. 2(a) demonstrates an ink-jet printed ITO pattern on a PET substrate where sharp line edges can be observed and the line width and interspacing also follow well our design. The SEM planar view of the printed line shown in Fig. 2(b) presents a porous and granulated structure which is frequently observed in nanoparticle films prepared by other techniques. The SEM cross-section view for 5 and 10 printing cycles respectively shown in Fig. 2(c) and (d) reveals that the film thickness is approximately proportional to the printing cycle and the film continuity is good enough for providing reliable conductance. The RMS roughness of the ink-jet printed film (5 printing cycles) measured by AFM as shown in Fig. 3 is ~44.6 nm. From the weight increased and the dimension (2 cm × 2 cm × 2.5 μm) printed, the estimated volume fraction of the printed ITO nanoparticles is approximately 33%.

Fig. 4(a) shows the optical transmittance of the films repeatedly printed with various printing cycles from 5 to 40 times. For 5 printing cycles (~2.5 μm, see Fig. 2(c)), the ITO film can approach ~80% transmittance in the visible region (400–800 nm). While the thickness increases, the optical transmittance rapidly decreases to a lowest value of ~30% in the visible region for 40 times printing. Generally, the transmittance in the visible region is found to slightly decrease with increasing film thickness for most deposited dense ITO films [2,3]. The great variation of the transmittance in the visible region with thickness as shown in Fig. 4(a) obviously results from the huge scattering effect of the aggregated nanoparticles as reported elsewhere [13].

It is worth to notice that only the specimen with 5 printing cycles presents a sharp absorption edge (around 330 nm) in contrast to other thicker films with broaden edges. According to the classic Mie theory [14] and the experimental results [15], for mono-dispersed small oxide nanoparticles, the absorption spectrum generally shows a clear and sharp absorption edge and the edge position sensitively varies with the particle size. In the present case, the sharp edge at 330 nm is quite close to the value found in the condensed ITO films [16,17] and the Mie calculation regarding an isolated 15 nm In_2O_3 nanoparticle [13]. For thicker nanoparticle films (over 10 printing cycles), strong scattering by the nanoparticle aggregates occurs over a very wide range especially in the visible region as discussed in Ref. [13]. This broaden scattering band almost fully covers the sharp band-gap absorption edge, and thus to have a broaden edge. This result suggests that the great scattering effect may be approximately ignored when the thickness of the nanoparticle films is below some critical values, i.e. ~2.5 μm in the present case.

For comparison purpose, we also introduce the normalized transmittance of mono-dispersed 15 nm ITO nanoparticles calculated by Mie theory. The calculated edge (slope and position at the very initial stage) is found to be similar to the experimental results of the deposited ITO dense films [2,3] but higher than our thicker ITO nanoparticle films. As a result, the overall optical behavior of the nanoparticle films still differs with that of deposited dense ones with similar thickness.

The electrical resistivities of the printed nanoparticle films are displayed in Fig. 4(b). The electrical resistivity rapidly decreases from 5 to 10 printing cycles and tends to reach a saturation value of ~200 Ω-cm after exceeding 20 cycles. By increasing printing cycle, the nanoparticle stacked films become denser and thicker, leading a formation of network between nanoparticles and providing more paths to transport free charge carriers. However, further increase in the film thickness does not effectively reduce the resistivity, which might result from the electron scattering from nanoparticle boundaries [18]. Joshi et al. results [4] show lower electrical resistivities in comparison with our data by using similar ITO nanoparticle (~15 nm) ink. But such difference is easy to be understood and acceptable due to their films were annealed at 300–800 °C which is not permitted for the present PET substrates. For conventional ITO films, it is generally not easy to inhibit the decrease of the electrical resistivity to a very low value of $\sim 10^{-4}$ Ω-cm with thickness increasing, but such ultrathin films also lead various drawbacks. The limited decrease of the resistivity of the present ITO nanoparticle films might be a merit for some specific applications, e.g. touch panels, which require a relatively high electrical resistance.

4. Conclusions

In this work, ITO nanoparticles were successfully synthesized and applied as the transparent conducting nanoparticle ink for the ink-jet printing technology. While the thickness of the printed ITO granulated film increases, the scattering effect caused by the nanoparticle aggregation and interfaces between nanoparticles is enhanced to affect the optical transmittance and spectra profiles. In addition, the electrical conductivity of the printed ITO films can be significantly improved by increasing film thickness up to a critical value.

References

[1] Wakeham SJ, Thwaites MJ, Holton BW, Tsakonas C, Cranton WM, Koutsogeorgis DC, et al. Thin Solid Films 2009;518:1355.
[2] Kim H, Gilmore CM, Piqué A, Horwitz JS, Mattoussi H, Murata H, et al. J Appl Phys 1999;86:6451.
[3] Kim H, Horwitz JS, Kushto G, Pique´ A, Kafafi ZH, Gilmore CM, et al. J Appl Phys 2000;88:6021.
[4] Joshi RN, Singh VP, McClure JC. Thin Solid Films 1995;57:32.
[5] Maruyama T, Fukui K. Thin Solid Films 1991;203:297.

[6] El Hichou A, Kachouane A, Bubendorff JL, Addou M, Ebothe J, Troyon M, et al. Thin Solid Films 2004;458:263.
[7] Granqvist CG, Hultåker A. Thin Solid Films 2002;411:1.
[8] Jeong S, Woo K, Kim D, Lim S, Kim JS, Shin H, et al. Adv Funct Mater 2008;18:679.
[9] Tekin E, de Gans BJ, Schubert US. J Mater Chem 2004;14:2627.
[10] Bühler G, Thölmann D, Feldman C. Adv Mater 2007;19:2224.
[11] Hong SJ, Kim YH, Han JI. IEEE Trans Nanotechnol 2008;7:172.
[12] Wohlmuth W, Adesida I. Thin Solid Film 2005;479:223.
[13] Lai HY, Chen CH, Lee CF. Plasmonics 2010;5:233.
[14] Link S, El-Sayed MA. J Phys Chem B 1990;103:4212.
[15] Liu Q, Lu W, Ma A, Tang J, Lin J, Fang J. J Am Chem Soc 2005;127:5276.
[16] Kim SS, Choi SY, Park CC, Jin HW, Cranton WM. Thin Solid Films 1999;347:155.
[17] Alam MJ, Cameron DC. Thin Solid Films 2002;420:76.
[18] Goebbert C, Bisht H, Al-Dahoudi N, Nonninger R, Aegerter MA, Schmidt H. J Sol-Gel Sci Technol 2000;19:201.